Supplementary material

"Human aging alters the neural computation and representation of space"
by Schuck, Doeller, Polk, Lindenberger and Li
NeuroImage

1. Boundary Vector Cell Model

For the boundary model, we started from a previous model that seeks to explain the sensitivity of place fields to changes in environmental geometry (Burgess and O'Keefe 1996). This so-called boundary vector cell (BVC) assumes that the hippocampal place cell system is provided with information about the distance between the animals' current position and the boundary in various directions. This information is carried by boundary vector cells, which have been identified in the rat subiculum (Lever et al. 2009). More technically, the BVC simulates place cell activity at a specific location as a summation of the activity of projecting boundary vector cells that are tuned to respond to the presence of a boundary in a specific direction and distance. Because each BVC signals the presence of a boundary in a particular direction and distance (its receptive field), a place cell should show maximum firing at the location where the given distance and direction to the boundary cause many projecting BVCs to fire. Since the original formulation of the BVC model was made for square environments, we extended the original model, which considered four directions in a *square* environment, to integrate an arbitrary number of BVCs in arbitrary directions in a *circular* environment. Specifically, we formulated a boundary distance function that calculates the distance of any arbitrary point **p** (within the boundary) to the boundary in any arbitrary direction θ as:

$$\Delta(r, \theta, \mathbf{p}) = r \frac{\sin \kappa}{\sin \delta} \quad (1)$$

where r is the radius of the circular environment, and δ and κ are defined by

$$\delta = \theta + \arctan2(x, y) + 90^\circ \quad (2)$$

$$\kappa = 180 - \delta - \arcsin\left(\frac{d}{r}\sin\delta\right) \quad (3)$$

In a nutshell, these calculations are based on trigonometric identities and reflect angles and side lengths of the triangle spanned between **p**, the center of the environment **m** and the point where the line from **p** in direction θ intersects with the boundary, **t**. A graphical depiction and further explanation can be found in Figure S1.

The firing at a given point **k** of a place cell with a place field centered at point **p** was then calculated as the summation of the activity of projecting 'boundary detectors' (BVCs), just as in Burgess & O'Keefe (1996):

$$f(\mathbf{k}) = \sum_{\theta} \frac{e^{\frac{-(\Delta(r,\theta,d_{\mathbf{k}}) - \Delta(r_0,\theta,d_{\mathbf{p}}))^2}{2\sigma^2(\Delta(r_0,\theta,d_{\mathbf{p}}))}}}{2\pi\sigma^2(\Delta(r_0,\theta,d_{\mathbf{p}}))} - T \qquad (4)$$

where r_0 is the radius of the environment in which the place field was established, r is the current environment's radius, T is a threshold and $\sigma(x) = w(2r^2 + \Delta(r_0, d_{\mathbf{p}}, \theta)) / 2r^2$ is a function that regulates the width of the tuning curves as a function of the distance from the boundary, with w being an arbitrary parameter that regulates the tuning width. As stated before, this function allows the incorporation of (summation over) an arbitrary number n of directions θ. In all simulations we used $n = 16$ directions, a w (tuning width) parameter of 5 and a threshold T of 80% of the maximum firing rate. The radii of the smaller, original and larger environment were 80, 100 and 120, respectively.

Because the modeled place fields have a number of complex properties which are untestable in the present experiment, such as size and shape of the place field, we formulated a simpler model that captures only the basic predictions (inward and outward shifts of place fields depending on boundary changes) but does not cover the more complex aspects (changed shapes of place fields), see main text.

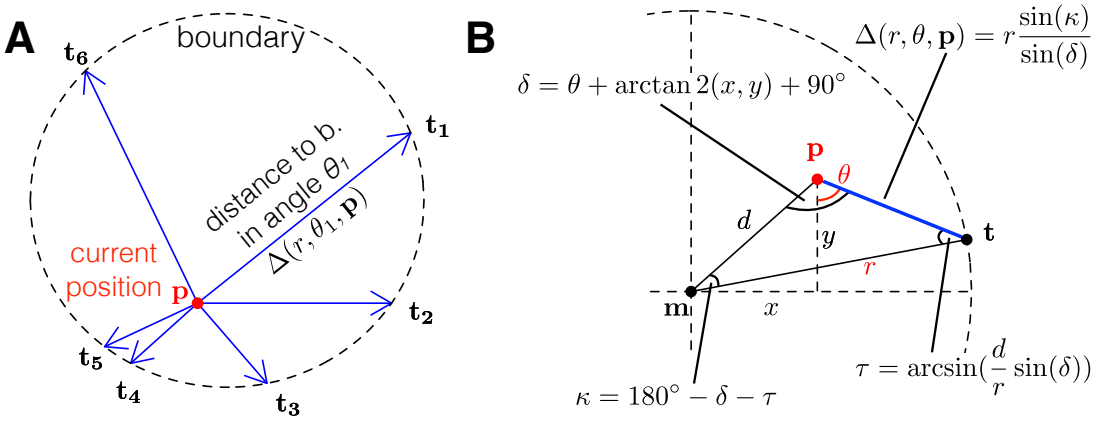

Figure S1: *Boundary vector model in a circular environment*. Panel A illustrates the boundary distance function. For a given point **p** (red) within the circular boundary, the function calculates the length of a vector that connects the boundary with **p** in direction θ (the blue arrows provide some examples). The intersection of this vector with the boundary is labeled **t**. (B) The calculation of the boundary distance function involves the triangle spanned by the points **p**, **t** and **m** (the center of the circle/environment). The illustration shows how different angles and the boundary distance function (here, length of blue line) are calculated when the coordinates of **p** (x, y), the radius r and the angle θ are given. The shown example assumes **m** to be (0, 0).

2. fMRI Preprocessing

Table S1: Preprocessing steps and parameters

Step	Parameter	Value
1. Create voxel displacement map (VDM) and unwarp EPI	Total EPI readout time	41.04ms
2. Realign	*Reference scan*	First image
	Image similarity metric	Least Squares
	Transformation	6 parameter rigid body Transformation
	Interpolation	B-spline 2nd degree
3. Coregistration	*Reference scan*	Mean Image
	Source image	T1 anatomical scan
	Image similarity metric	Normalized Mutual Information
4. Segmentation into white and gray matter	*Algorithm*	SPM 8's New Segement
	Brain image template	SPM8's MNI templates
5. Normalization	*Template*	Study Specific DARTEL template
	Deformations	DARTEL Flow field
	Size	3 X 3 X 3 mm
6. Smoothing	*FWHM*	8 mm

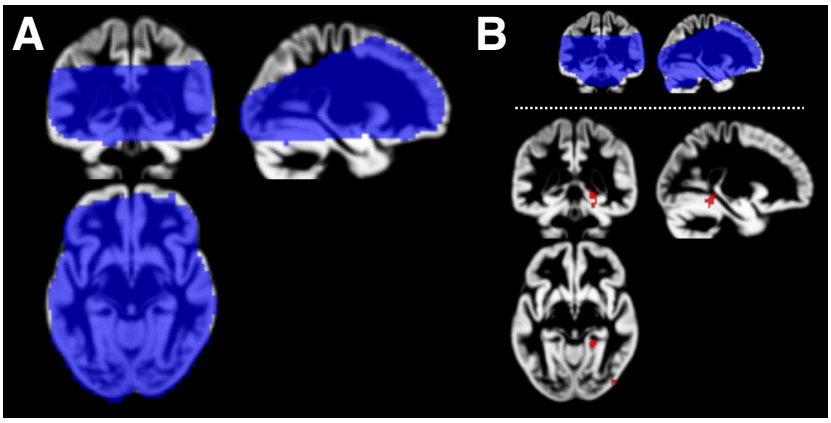

Figure S2: *Whole brain coverage of all group analyses*. (A) Covered brain areas for main analyses shown in blue. Signal loss lead to impaired coverage in anterior hippocampus. (B) To check whether the signal loss in anterior hippocampus led to masking of results, we manually excluded five participants whose signal caused major anterior hippocampus signal loss. This resulted in more coverage of anterior parts of hippocampus (upper panel). Repeating the model X age group interaction test (lower panel), however, largely replicated your results, and did not show activation in anterior hippocampus

3. fMRI Results

Table S2: Age Differences in Activation for the Cue vs. Baseline Contrast.

			MNI Coordinates		
Region	*Laterality*	*Z*	*x*	*y*	*z*
Younger > Older					
Hippocampus	L	4.03	-24	-36	12
	L	3.93	-30	-39	3
Older > Younger					
Middle Temporal Gyrus	R	5.89	60	-42	9
	L	5.72	-54	-51	12
Middle Frontal Gyrus	R	5.25	48	6	54
	L	3.98	-30	48	12
	L	3.78	-27	36	30
Supplementary Motor Area	R	4.64	6	6	63
	L	4.23	-6	6	60
Middle Cingulate Gyrus	R	4.32	9	15	39
	R	3.47	3	-27	51
	L	3.63	-9	-30	42
Caudate Nucleus	L	5.41	-12	15	-3
Inferior Frontal Gyrus	R	4.95	45	21	9
Inferior Temporal Gyrus	R	3.72	48	-57	-15
Precentral Gyrus	L	5.29	-45	-6	30

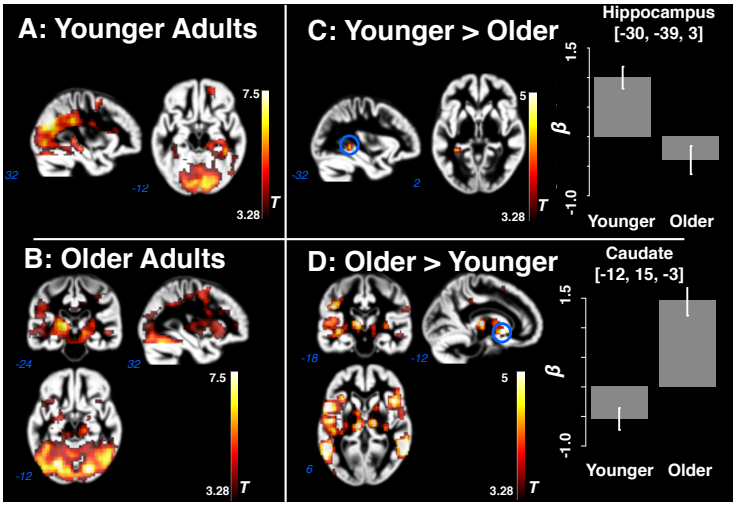

Figure S3: *Brain activations during the cue display*. All activation maps show color-coded T values overlaid on the study specific gray matter template. (A + B) Younger and older participants activated a large network of areas including the cerebellum, occipital cortex, retrosplenial cortex and motor areas. (C) Compared to older adults, younger adults showed greater activation in the left posterior hippocampus. (D) Older adults showed greater activation in a variety of areas, including the left caudate nucleus. Barplots show the contrast estimates in the hippocampal and caudate nucleus peak regions.